UNITED NATIONS UNIVERSITY
GEOTHERMAL TRAINING PROGRAMME
Orkustofnun, Grensásvegur 9,
IS-108 Reykjavík, Iceland

Reports 2011
Number 15

FLUID CHEMISTRY, FEED ZONES AND BOILING IN THE FIRST GEOTHERMAL EXPLORATION WELL AT MENENGAI, KENYA

Jeremiah Kipng'ok
Geothermal Development Company – GDC
P.O. Box 17700 – 20100
Nakuru
KENYA
jkipngok@gdc.co.ke

ABSTRACT

Exploration drilling to prove steam in the Menengai volcanic system started in February, 2011. A total of four wells have so far been drilled in an ongoing drilling program and the first well, MW-01, has been discharging for over 4 months. Flow tests, pressure and temperature logs, and chemical data from the first well have been used to determine the chemical and physical characteristics of the well. The findings establish that four aquifers of varying temperatures are the main permeable horizons penetrated by the well. Quartz and Na/K equilibrium temperatures indicate that a large component of well MW-01 discharge constitutes fluids withdrawn from the shallowest and coolest feed zone. The flashed geothermal water from the well is rich in CO_2 and high in Na concentrations with relatively high Cl values (>500 ppm). The high CO_2 appears to be source controlled, i.e. by flux from the magma. High CO_2 partial pressures are observed around the aquifers feeding the well. These high gas pressures considerably lower the boiling point of the rising hot water, reflecting lower boiling temperatures for the measured total pressures in the well. Low calcium concentrations were noted in the discharged water from the well which may be due to the removal of Ca from the aquifer solution by calcite precipitation. The waters in the well indicate strong over-saturation with respect to calcite.

1. INTRODUCTION

Menengai geothermal field is situated on the axis of the central segment of the Kenya rift valley. The Kenya rift is part of the eastern arm of the East African Rift System, an active intra-continental divergence zone. It is a volcano-tectonic feature that transects the country from Lake Turkana in the north to Lake Natron (Tanzania) in the south. It is a host to several Quaternary to Recent volcanic complexes (Simiyu, 2010; Omenda, et al., 1993; Riaroh and Okoth., 1994). This segment has a high thermal gradient which is due to shallow intrusions, and the volcanic centres that exist are associated with active geothermal systems.

A detailed geo-scientific assessment of the Menengai field was conducted to ascertain the geothermal potential of the area. Integrated results of the studies indicate the existence of a hot, ductile, and dense

body centred under the Menengai caldera. Modelling indicates that the hot magmatic body resulted in the formation of a geothermal system under the Menengai caldera with the upflow within the caldera and outflows to the north (Lagat et al., 2010; Mungania et al., 2004). This culminated in the sinking of the first deep exploration wells in February, 2011 in an ongoing exploration drilling program to prove steam.

2. GEOLOGY OF MENENGAI

2.1 Location

The Menengai geothermal field is located north of Lake Nakuru and south of Lake Bogoria (Figure 1). It encompasses the Menengai volcano, the Ol'Rongai volcanoes, Ol'Banita plains and parts of the Solai graben to the northeast. It is situated at the triple junction between the main Kenya rift and the less prominent Nyanza rift.

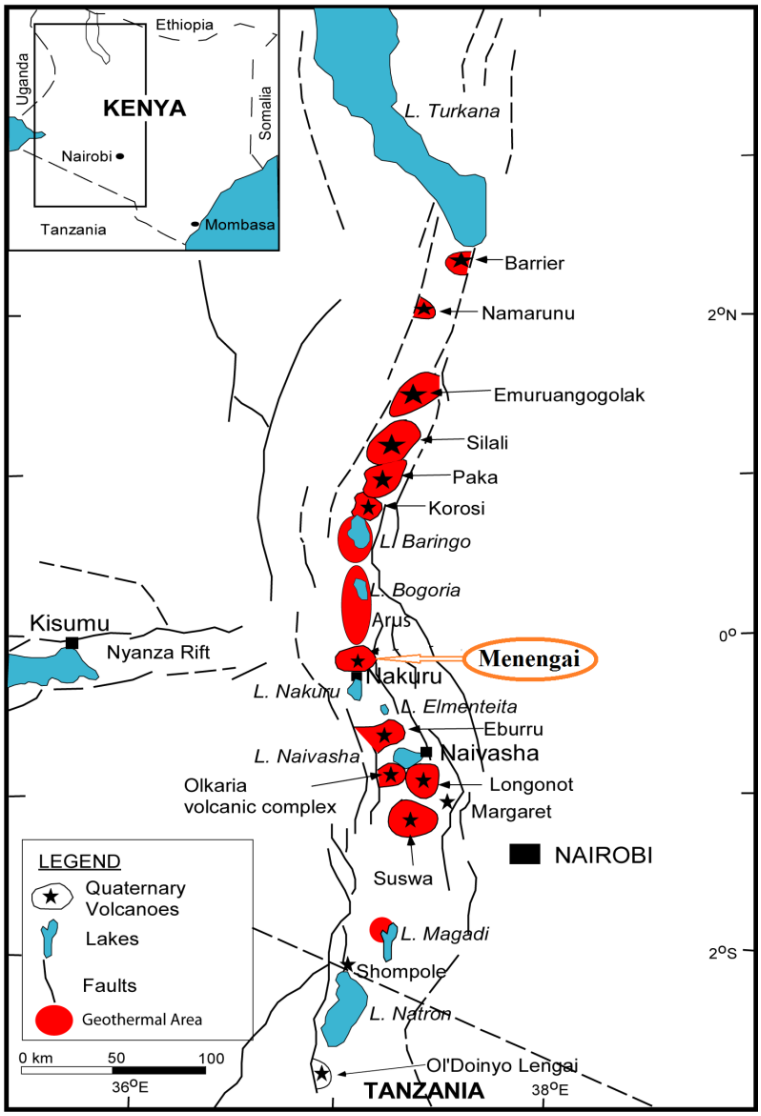

FIGURE 1: Map showing location of Menengai and other geothermal areas in Kenya (modified from Ofwona et al., 2006)

2.2 Surface geology

A number of studies have been carried out in the Menengai geothermal area for varying objectives and its geology has been described by many authors (Jones and Lippard, 1979; Leat, 1984; Leat, 1985; Macdonald et al., 1994; Geotermica Italiana Srl, 1987; Williams et al., 1984). Menengai is a late Quaternary volcano which has produced trachyte and pantellerite volcanics. They comprise pyroclastics and lava flows with most of the surface adjacent to Menengai caldera being covered by extensive pyroclastics, which accompanied the collapse of the caldera (Lagat et al., 2010; Mungania et al., 2004). Young lava flows infilling the main caldera are post caldera in age. Older (Pleistocene) lavas, mainly trachytic and phonolitic in composition, are exposed in the northern parts and are overlain by eruptives from Menengai volcano. The Menengai shield building lavas consist mainly of trachytic lavas and minor sheet and cone forming pyroclastics. The lowest trachyte lava yielded a date of 0.18+0.01 ma (Leat et al., 1984).

The Menengai geothermal area is characterized by young volcanism represented by numerous recent eruptions both inside and outside the caldera, the large caldera collapse and intense tectonics resulting in faults marking the area. The surface is covered by volcanic rocks, mostly erupted from centres within the area. Most of the area around the Menengai caldera is covered primarily by pyroclastics

erupted from centres associated with the Menengai volcano. Leat et al. (1984) noted that the Menengai volcano seems to be composed entirely of per-alkaline Si-oversaturated trachytes. The main rock units exposed in and around the Menengai area can be generally classified into pre-caldera, syn-caldera and post-caldera volcanics according to their age. The Menengai shield building lavas exposed on the Menengai caldera cliffs form the pre-caldera rocks. They consist mainly of trachytic lavas and minor sheet and cone forming pyroclastics. The syn-caldera volcanics are mainly pyroclastics, which are contemporaneous with the 77 km^2 (12 x 8 km) cauldron collapse. The rock units comprise extensive air fall tuffs, ignimbrite and some lithic tuffs. Geotermica Italiana Srl (1987) published an age of 14,900±900 yrs based on carbon dating of palaeosoils between the syn-caldera eruptives. All post-caldera eruptives are trachytes and pantellerites. They mostly comprise blocky and ropy lava flows, some sub-plinian air-fall tuffs and cinder cone material. Over 70 lava flows have been counted on the caldera floor (Leat et al., 1984). An age of 1,400 yrs for the post-caldera lavas is published by Jones and Lippard (1979). Other rocks exposed in the adjacent area are the Pliocene volcanics which are exposed away from the main Menengai volcanic pile.

Surface hydrothermal activity is manifested in this area by the occurrence of fumaroles, warm springs, steaming/gas boreholes, hot/warm water boreholes and altered ground. Fumaroles are located mainly inside the caldera floor; a few inactive ones occur in the Ol'Rongai area, primarily controlled by the Molo Tectono-volcanic axis (TVA).

2.3 Structural geology and hydrogeology

The major structural systems in the area are the Menengai Caldera, the Ol'Rongai Tectono-volcanic axis and the Solai graben. The floor of the Menengai caldera depicts extensional tectonics with the main trough trending N-S north of Menengai and NNW-SSE south of Menengai. This sharp trend change is associated with the extent of Cambrian craton/orogenic belt contacts (Simiyu and Keller, 1997). The Menengai caldera is an elliptical depression with minor and major axes measuring about 11.5 km and 7.5 km, respectively. The circular rim of the caldera ring fault is well preserved with vertical cliffs at some places measuring up to about 400 m. The ring structure has been disturbed only by the Solai graben faults in the NE end and a fracture at the SSW end.

The Ol'Rongai structural system represents a part of the larger Molo TVA (Geotermica Italiana, 1987) that has had a lot of volcanic activity, including eruptions, resulting in a build-up of a NNW trending ridge referred to as Ol'Rongai volcanoes. Over the Ol'Rongai area, the structure is marked by intense volcanic activity including explosive (pumice issuing) craters. This part of the structure is adjacent to the Menengai caldera. It is possible that this structure extends into the Menengai caldera.

The Solai tectonic axis is a narrow graben averaging 4 km in width that runs in a N-S direction from the eastern end of Menengai caldera, through Solai. It is comprised of numerous faults/fractures all trending in a N-S direction. This is the only system that has cut the Menengai pyroclastics. The southern extension under the Menengai volcanic pile is an important hydrogeological control and a possible permeability enhancement of brittle lava formations underlying the Menengai eruptives.

The hydrogeology of the area is mainly inferred from data obtained from water boreholes. Information on aquifer properties and groundwater flow patterns is provided by interpretation of data from these boreholes, the majority of which were drilled to 100-200 m depth. However in the caldera floor, greater reliance is placed on indirect methods of assessing recharge, e.g. surface hydrological information due to a paucity of borehole data. The relative yields of the boreholes may be matched with the petro-physical property of the feeder formations, which range from dry and thermally anomalous boreholes to very high yield boreholes (>20 m^3/h). The dry and elevated temperature boreholes are distributed along the Molo TVA that extends from the Menengai caldera northward through the Ol'Rongai volcano, Lomolo and Gotuimet volcano. The high yield boreholes are located to the east of the caldera and are bound by the Bahati and Marmanent scarps which are relatively

wetter and on higher grounds. Earlier studies have shown that these areas are fed by channels along the rift scarp faults.

2.4 Lithology

Borehole data for Menengai well MW-01 indicate that the well penetrates rocks predominantly composed of quartz normative and silica over-saturated peralkaline trachytes. They are mainly fine to medium grained pantelleritic trachytes with minor intercalations of tuffaceous materials in zones of vein fillings.

3. EXPLORATION DRILLING

Kenya is endowed with vast geothermal resources, along the axis of the Kenya rift, estimated from exploration studies to be in excess of 7,000 MWe (Simiyu, 2010). Until 2010, only Olkaria and Eburru had proven geothermal systems while other prospects were still at varying exploratory stages. Menengai is considered one of the high potential geothermal prospects in Kenya while being strategically located due to its proximity to power transmission lines and a populated town. Prior to committing the field for exploratory drilling, detailed surface exploration was carried out by KenGen in collaboration with the Kenya Ministry of Energy (Mungania et al., 2004) and later infill work by Geothermal Development Company (Lagat et al., 2010).

The surface exploration findings showed positive indications of the existence of a geothermal resource in the Menengai area that could be commercially exploited. Active fumaroles inside the Menengai caldera and the morphological build-up of a lava pile dome inside the caldera floor by very young lavas, form strong evidence of the existence of an active magma chamber below Menengai. Geophysical surveys revealed that the heat source for the Menengai prospect is associated with a hot magmatic body (Young et al., 1991; Simiyu and Keller, 2001) that underlies the caldera structure at Menengai; a similar heat source is likely to be associated with the Ol'Rongai and Ol'Banita geothermal areas. The central part of the caldera, the Ol'Rongai area and the western domain towards Kabarak, which is separated from the central one by a structural discontinuity, show a low resistivity (< 10 Ωm) anomaly at depth. Joint TEM and MT soundings infer that the potential area of an inversion resistivity anomaly is about 107 km^2 which could yield over 1,600 MWe based on the world's average of 15 MW/km^2.

Subsurface temperatures in excess of 270°C have been predicted in Menengai using geothermometers based on gas compositions of the sampled fumarole discharges. Surface heat loss studies indicated that massive heat is lost in the area, with the Menengai caldera representing a substantial component of it. This high heat flow from the caldera could be indicative of a huge hot body underneath which should be explored for steam production. Areas around Ol'Rongai and Ol'Banita indicated low heat flow. The low heat flow could be due to the fact that they are older systems. Subsurface structures were also mapped from CO_2 and radon soil gas anomalies.

The results from the geoscientific exploration were integrated to develop a conceptual model of the geothermal system in Menengai, and exploration well sites were subsequently proposed (Figure 2). Exploration drilling in Menengai started in February, 2011 with the sinking of the first well, MW-01. The surface hole diameter of well MW-01 is 26″ and was cased using a 20″ casing to a depth of about 80 m. A 17 ½″ intermediate hole was drilled to a depth of 400 m and cased using 13 ⅜″ casing. A 12 ¼″ production hole was drilled to about 850 m depth and cased to the surface using a 9 ⅝″casing. An 8½″ main hole was then drilled to a depth of around 2200 m and 7″ slotted liners were run in.

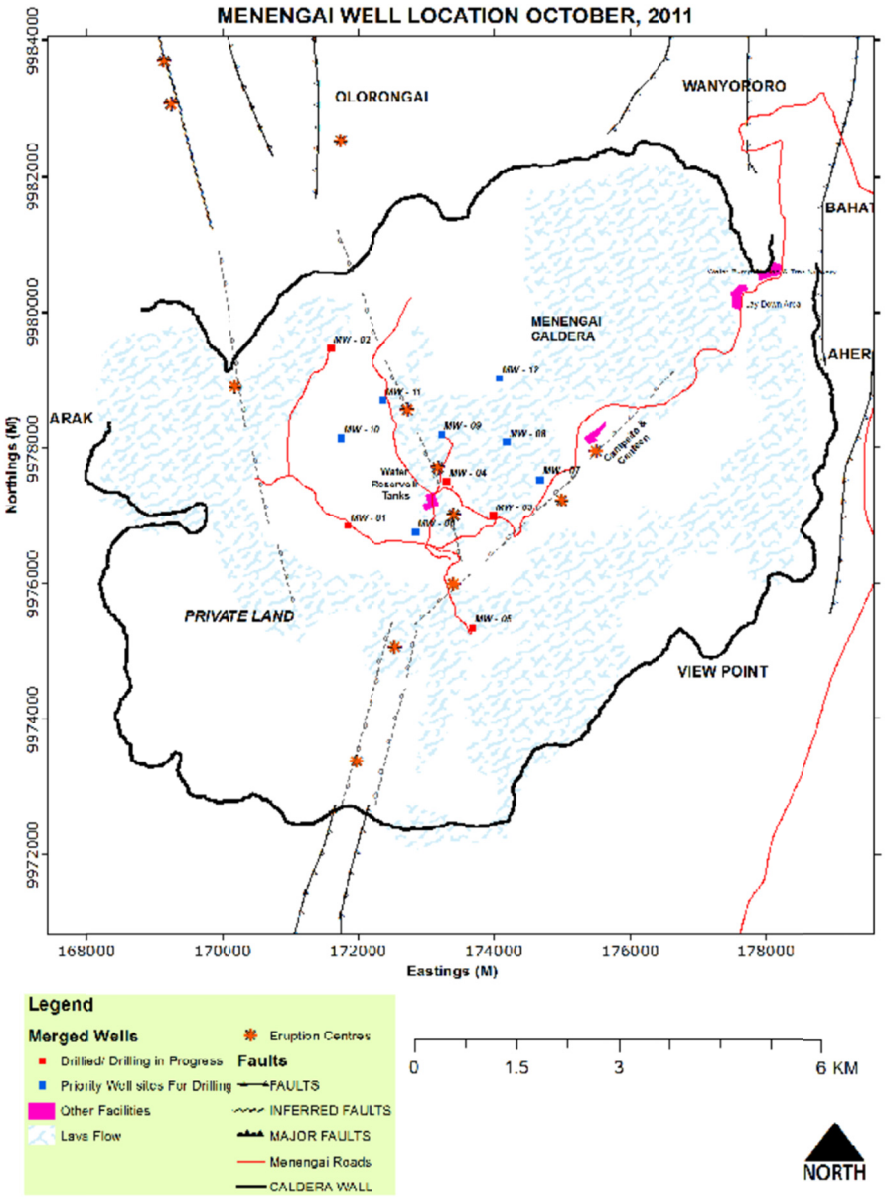

FIGURE 2: The Menengai geothermal area map showing the location of drilled and proposed exploration wells (from GDC, 2011)

4. WELL CHARACTERISTICS

4.1 Flow tests

Menengai exploration well MW-01 was completed on May 1st 2011. The well was discharged vertically on May 12th to May 18th. The next flow test started on May 25th and is still ongoing. When this second flow test started, the well had not recovered thermally. Wellhead pressure was monitored and total discharge and enthalpy were obtained by the critical lip pressure method by measuring critical lip pressure and water flow from the weir box. The measurements are still ongoing at the time of writing this report. Some of the results are displayed in Table 1 along with the chemical data. Total mass flow ranged from 44 to 62 kg/s while steam flow values fluctuated within 10 and 16 kg/s at a wellhead pressure of 7-14 bar abs. Discharge enthalpy values range between 1040 and 1250 kJ/kg. The steam flow is equivalent to about 5.6 to 8.9 MWe.

4.2 Sampling and analysis

Steam and water samples for the first set of analyses used in this report were collected with the aid of a webre separator. The webre separator was connected to a horizontal two-phase flow pipe between the wellhead and the atmospheric silencer at distance of 1.5 m from the wellhead. The sampling conditions are those described by Arnórsson et al. (2006). The water sampled was cooled at the point of sampling by passing it through a stainless steel coil to prevent boiling. Steam samples were collected in 325-340 ml evacuated gas sampling flasks containing 50 ml of 40% w/v NaOH solution. The gas sampling bulbs were weighed before and after sampling to record the amount of steam condensate collected. Water samples were collected and treated in the following ways: Raw and untreated samples were collected in 500 ml bottles for determination of pH, conductivity, total dissolved solids (TDS), total carbonate carbon (TCC), Cl, F and B. Samples for silica analysis were collected in 150 ml bottles and diluted ten times. Samples to be analysed for cations and SO_4 were filtered through a 0.45 μm millipore membrane and 1 ml of concentrated nitric acid was added to the cation samples while 1 ml of 0.2M zinc acetate solution was added to the samples for sulphate analysis to fix sulphides. Subsequently, the zinc sulphide precipitate was filtered from the solution. All the bottles used for sampling are of polyethylene material.

Steam samples were analysed for CO_2, H_2S, CH_4, H_2, N_2 and O_2. Analysis of CO_2 and H_2S was done titrimetrically using 0.1 M HCl and 0.001M mercuric acetate, respectively. Non-condensable gases (CH_4, H_2, N_2 and O_2) were analysed by gas chromatography. Analysis of H_2S in the water samples was done on site in the same way as the steam samples. TCC in the water samples was also determined the same way as was done for steam samples. Measurements of pH, TDS and conductivity together with TCC analysis were carried out in the laboratory at room temperature (20°C), a few hours after sampling. Correction for interferences from other bases in the analysis of total carbonates was not done. Analysis of B, SiO_2 and SO_4 were done spectrophotometrically using UV/VIS while the major aqueous cations (Na, K, Ca, Mg, Al, Fe) were determined using ICP-MS after multi-dilution. Chloride analysis was done titrimetrically using Mohr's method while fluoride was analysed using ISE. The chemical results for both water and gas analyses are given in Table 1. The reported TCC concentrations in Table 1 would be low if some degassing of the samples occurred before they were analysed.

The water pH as measured at 20°C ranges between 9 and 9.3. The pH of the water samples may be affected by various processes subsequent to collection. An accurate pH measurement is of major importance for reliable geochemical interpretation. Assessment of the state of mineral-solution equilibria in the aquifer and mineral-gas equilibria involving $CO_{2,\,aq}$ and H_2S_{aq} is affected by aquifer water pH due to its effect on the relative concentrations of the carbonate and sulphide-bearing species (Karingithi et al., 2010). The reported pH values for well MW-01 waters may be high considering the high dissolved total carbonates in the waters. The calculated CO_2 partial pressure of the samples is similar to the CO_2 partial pressure of the atmosphere. This implies either that the samples had lost or gained CO_2 to/from the atmosphere to attain equilibrium or, alternatively had P_{CO2} equal to that of the atmosphere at the time of sampling. This is further compounded by the type of sampling bottles used; as can be noted from sample collections, air-tight glass sampling bottles were not used. Assuming that both the analysis of pH and TCC are reliable, this indicates that little CO_2 gas is present in the sample and almost all of the TCC is present as HCO_3^-. If this is the case, the reported analytical concentrations of other major anions and cations must be in large error to explain the ionic imbalance of the samples. Also, the measured pH values may be high as a result of silica polymerization upon sample storage. The polymerization reaction involves the extraction of $H_4SiO_4°$ from the solution. In waters with high pH (above 9), like that from well MW-01, a high proportion of ionized silica ($H_3SiO_4^-$) relative to unionized silica exists, implying that the extraction of $H_4SiO_4°$ from the solution will cause an increase in pH.

TABLE 1: Chemical analysis results of water and steam samples from Menengai well MW-01; component concentrations for water samples are in ppm and mmol/kg for steam samples

					Water samples																	Gas samples					
Date of sampling	Sample ID	WHP[a] bars	GSP[b] bars	h[d] kJ/kg	Diss. Solids	pH[m]	pH[c]	B	SO_4	Cl	CO_2	F	H_2S	SiO_2	Al	Ca	Li	Na	K	NH_4	Mg	Fe	CO_2	H_2S	CH_4	H_2	N_2	O_2
25-May-11	592	3.4	0.8	1037	6970	9.2	6.3	0.05	262.9	704	6189	143	34	300	0.20	1.0	1.3	2300	211	10.4	0.002	0.001	1425	3.5	3.9	14.4	25.8	0
26-May-11	593	7.2	1.0	1141	6725	9.2	6.2	0.33	306.8	715	6118	155	27.2	327	0.25	0.8	1.2	2193	250	12.8	0	0.018	1452	4.4	4.1	14.8	28.3	0
27-May-11	594	7.6	1.4		6460	9.1	6.2	0.10	285.7	718	6354	154	20.4	255	0.27	1.0	1.6	2221	227	12.4	0	0	1407	6.5	1.2	38.3	11.6	0
30-May-11	595	7.2	0.1	1184	6765	9	6.4	0.20	220.3	711	6472	149	19.4	261	0.21	1.0	1.4	2537	240	12.3	0	0	1181	4.3	5.8	37.6	15.0	0
31-May-11	596	7.2	0.1	1199	6750	9.1	6.3	0.10	217.8	656	6895	157	20.4	263	0.25	1.2	1.2	2434	238	11.7	0	0.014	1145	3.9	3.5	22.8	7.7	0
2-Jun-11	597	7.2	0.7	1128	6730	9.2	6.3	0.17	216.5	806	6545	152	20.4	323	0.20	0.9	1.3	2468	228	11.1	0	0	1236	12.3	2.2	14.4	4.2	0
3-Jun-11	598	7.2	0.1	1158	6955	9.1	6.3	0.13	212.4	775	6589	155	37.4	283	0.21	0.9	1.3	2365	217	20.0	0.005	0	1251	12.5	4.3	28.1	7.9	0
6-Jun-11	599	7.2	0.2		7245	9.1	6.1	0.10	213	782	6646	158	37.1	320	0.27	1.2	1.7	2180	200	12.9	0	0	888	5.9	2.3	17.2	3.5	0
7-Jun-11	600	7.6	0.3	1134	7095	9.1	6.3	0.17	228.9	648	6758	158	36.7	289	0.23	1.2	1.1	2517	227	12.8	0	0.001	835	10.4	3.5	22.2	4.1	0
8-Jun-11	601	7.6	0.1	1176	7220	9.1	6.4	0.20	214.7	743	6972	154	16.3	343	0.22	1.0	1.5	2724	245	12.2	0	0	902	13.3	2.4	15.5	2.6	0
9-Jun-11	602	7.6	0.1	1130	6965	9.3	6.3	0.13	201.3	842	6626	166	39.1	342	0.26	1.1	1.9	2488	222	11.3	0	0.004	991	13.4	4.1	26.2	4.5	0
10-Jun-11	603	7.6	0.1	1170	7110	9.1	6.2	0.03	218.3	690	7198	156	41.0	321	0.28	1.2	1.8	2434	210	11.6	0	0.018	1020	15.5	4.6	29.0	2.9	0

[a] Wellhead pressure; [b] Pressure at which steam samples were collected; [c] Calculated pH
[d] Discharge enthalpy; [m] Measured pH

4.3 Feed zones

Knowing the depth level of feed zones or permeable horizons is essential in determining the possible main source of fluids issuing from geothermal wells. This information is also crucial for well design, plans for deviated drillings and deciding on well spacing. A correlation between the lithology and permeable levels in the wellbore also provides an understanding of reservoir characteristics. Loss of circulation of drilling fluid, temperature and pressure logs during thermal recovery of the well and geothermometers have all been used to locate these permeable horizons. In addition, CO_2 partial pressures have been used to map inflow zones. This is a new method made possible by the high CO_2 in the well fluid.

4.3.1 Circulation losses

Information on drilling fluid returns was obtained from the drilling history of the well and is displayed in Table 2 below.

TABLE 2: Drilling fluid returns/losses

Depth (m)	Remarks/comments
1077-1078	Loss of circulation
1247-1342	Partial returns at times
1739-1786	No returns
1842-1843	No returns
1739-1952	Intermittent returns
1952-2184	Intermittent returns
1988-2007	Loss of circulation
2031-2059	Loss of circulation
2124	Loss of circulation

The losses of drilling fluid during drilling are shown in Table 2; these losses do not all necessarily represent permeable horizons. Losses of circulation may occur as a result of the reopening of aquifers at higher levels in the well. This is particularly prone to occur when pumping of the drilling fluid is halted temporarily when drill rods are being added to the drill string.

4.3.2 Temperature and pressure logging during thermal recovery

Downhole temperature and pressure measurements were carried out during the heat-up of well MW-01 after well completion and the results are shown in Figure 3.

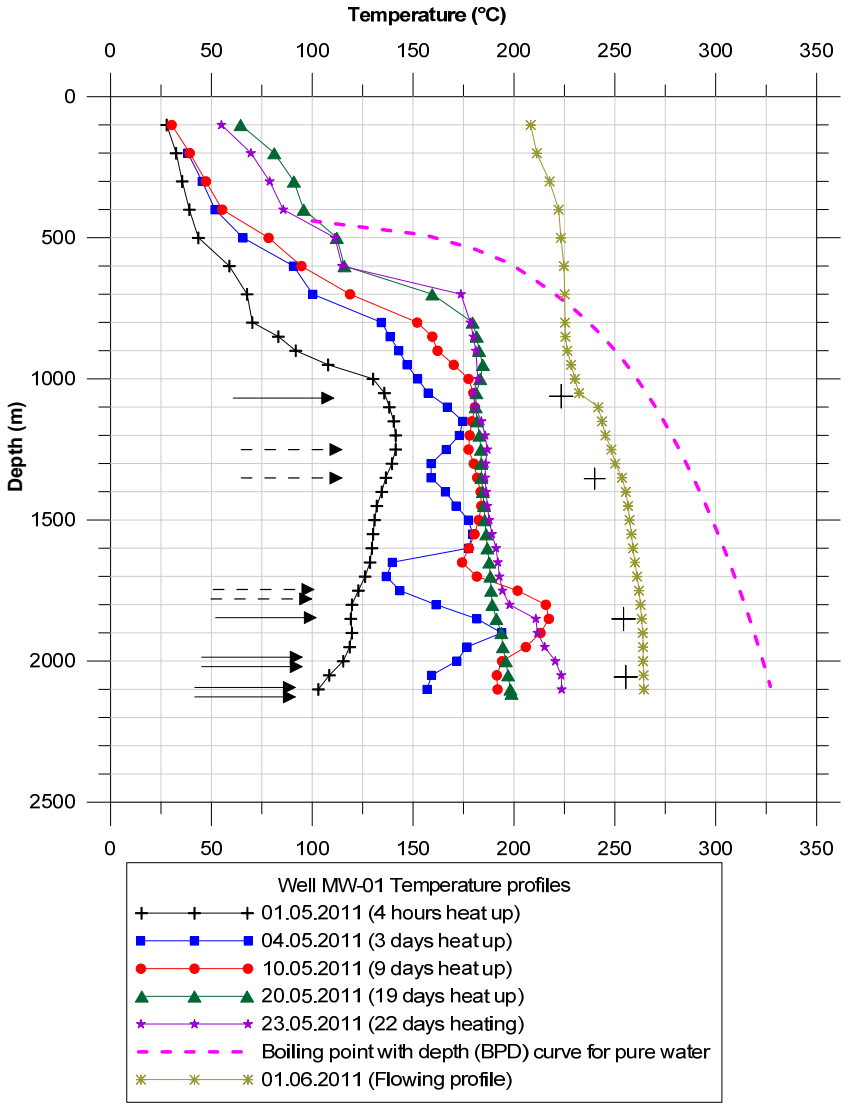

FIGURE 3: Well MW-01 temperature profiles. Arrows indicate depths where loss of circulation fluid during drilling was encountered; crosses indicate feed zones

The temperature and pressure recovery surveys indicate the existence of multiple feed points. A major feed zone was encountered at around 1050 m depth. This was also affirmed by the geothermometer temperatures which suggested that a large portion of the liquid discharged at the wellhead issues from this horizon. Another permeable horizon was observed at about 1340 m depth (9 day profile). The feed zone at this horizon however, appears to be minor. At 1850 m depth, a significant rise in temperature is evident (3, 9 and 22 days profiles). This indicates another major aquifer located at this horizon. Near the well bottom (2050 m depth), there appears to exist another permeable horizon (22 day profile). Enhanced loss of drilling fluid was experienced at this horizon as well. It is, however, important to note that the wellbore has not reached thermal stabilization at the time of the latest temperature run.

The boiling point of pure water with depth for well MW-01 has been computed from the water rest level in the well. A depth of about 440 m was estimated from the pressure logs. The shut-in temperature logs showed lower temperatures, deviating from the boiling point curve for pure water with depth by as much as 100°C at well bottom (22 days heat up graph). The shift in temperature is attributed to the effects of gas pressure. Generally, temperatures frequently follow the boiling point curve closely for pure water with depth as revealed by extensive studies of many drilled geothermal fields (Stefánsson and Björnsson, 1982). However, dissolved gases in the geothermal water, as is exemplified in MW-01, affect the boiling point depending on their concentrations (Arnórsson, 1985). When the sum of steam pressure and total gas pressure equals hydrostatic pressure for the rising thermal water, it begins to boil. It is observable that well MW-01 has significant gas present in the inflowing fluid into the well. The effect of gas partial pressures on temperature in Menengai well MW-01 is clearly illustrated in Figure 5.

Downhole pressure profiles taken during well thermal recovery are presented in Figure 4. The graphs depict the pressure control points in the well. The pressure pivot or pressure control point concept is crucial to understanding well behaviour during the heating up period (Grant and Bixley, 2011). A well's pivot point is defined as the point at which the well pressure equals the formation pressure. In a

well with several feed zones as is the case with Menengai well MW-01, the pressure may pivot at a depth between the different permeable horizons in the well. This is because the depth of the pivot point in the well is influenced by the permeability of each zone and the characteristics of the well and formation pressure. Grant et al. (1983) discussed the identification of internal flows in the wellbore and the effect of these on pressure. He reasoned that where there are multiple feeds, intermediate ones may be hidden, and the pivot point may reflect the inflows and outflows of the extreme points alone. The pressure profiles pivot slightly below the production casing depth (880 m) for MW-01 but appear to be shifting downhole to 1850 m as the well continues to thermally recover. Pressure measurements taken during discharge (Figure 4) for this well show that boiling starts in the formation beyond the well bottom.

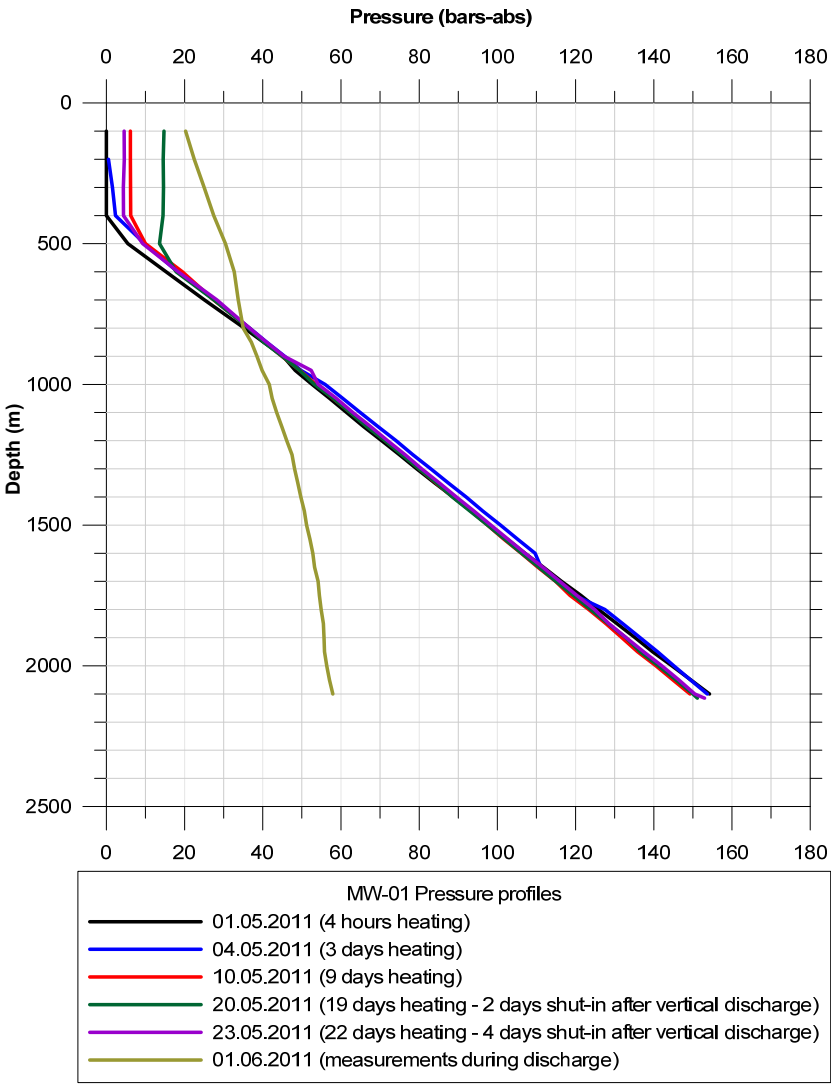

FIGURE 4: Pressure profiles for well MW-01. Measurements during discharge indicate a two-phase flow in the well from the well bottom

4.3.3 CO_2 partial pressure

Calculation of gas pressures in individual feed zones would require modelling of the contribution of each zone to the well discharge. Such geochemical modelling has not yet been developed. As a first approximation, aquifer fluid compositions were computed for the present study at two different temperatures, one corresponding to the feed at 1050 m depth and the other at the deep feed at 1850 m. The WATCH program (Arnórsson et al., 1982) version 2.4 (Bjarnason, 2010) was used for these calculations. For the upper feed zone, the aquifer temperature was taken to be 190°C but 265°C for the feed at 1850 m depth. Calculated pressure for pure water at different temperatures and the measured downhole pressure during discharge have been plotted and are presented in Figure 5.

The graphs in Figure 5 indicate that there are four main feed zones, at around 1050 m (42.4 bars), 1300 m (48 bars), 1800 m (54.9 bars) and 2050 m (57 bars) depths. The difference between the measured P-T curve and the curve for pure water represents gas pressures. Apparently, gas pressures increase at depth levels where the well intersects shallower feed zones. The cause of this increase could either be higher gas content of the fluid in shallower feed zones or that the fluid in these feed zones contains a small steam fraction and, therefore, gaseous steam at the point of inflow into the well. At the deepest aquifer, gas pressure during discharge amounts to 8-9 bars but, at the shallowest aquifer it is almost 13 bars. At the wellhead (20 bars), the gas content of the steam is about 1.6 bars. The

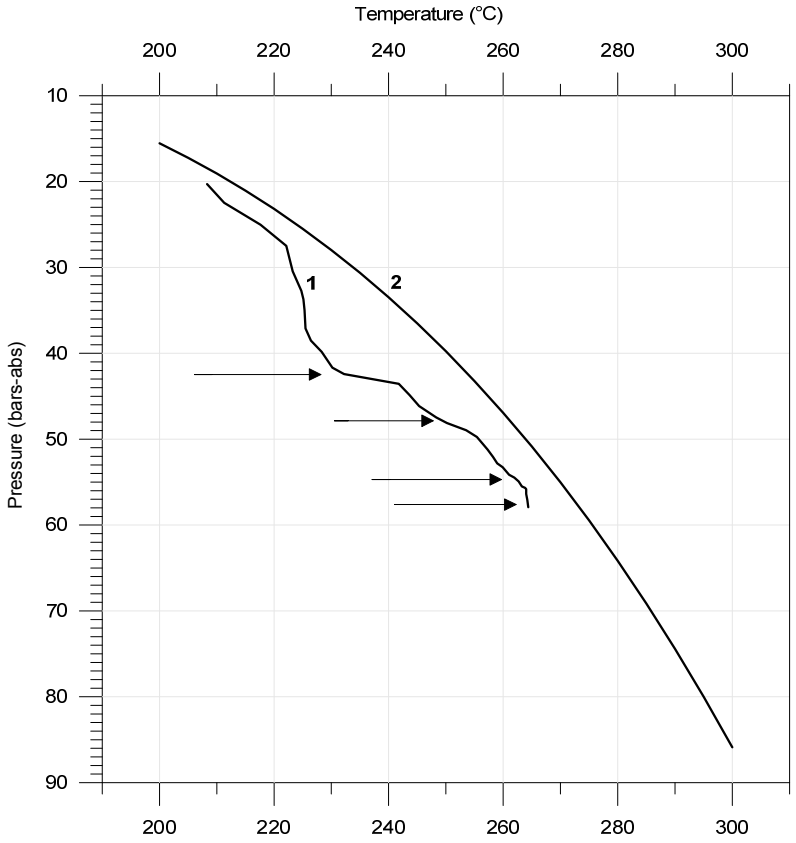

Figure 5: Pressure at measured and calculated temperatures; Curve 1: Measured temperature and pressure (hydrostatic) during discharge of well MW-01; Curve 2: Temperature and pressure of saturated vapour for pure H_2O; Arrows indicate aquifers. The main feed zones are likely the shallowest and the deepest ones.

lower gas pressure at the wellhead is due to the fact that the early formed steam is relatively enriched in gas but further boiling of the water adds nearly gas-free steam to the vapour phase and, thus, decreases its gas concentrations. It is observed that CO_2 accounts for almost all of the gas content, as deduced from the chemical analysis of the steam phase. The gas pressure of 1.6 bars at a vapour pressure of about 20 bars indicates that CO_2 is 8% of the vapour by volume. CO_2 partial pressures in the initial liquid water beyond the depressurization zone around the well are likely to be on the order of 20-30 bars.

4.3.4 Geothermometer temperatures

Downhole temperature logging in wells only gives reliable information on the earth's subsurface temperatures if there is no internal flow between permeable horizons, as well as no inflow of steam from two-phase aquifers. Geothermometers, on the other hand, provide information on the temperature of feed zones in the well and, in the case of two or more feed zones, as is observed in well MW-01, an intermediate temperature is attained. However, if the temperatures of the feed zones vary significantly, it may show up as discrepancies between geothermometers. In this paper, aquifer temperatures for Menengai well MW-01 were computed by quartz (Fournier and Potter, 1982) and Na/K (Arnórsson et al., 1983) geothermometers. The application of quartz and Na/K geothermometers to high temperature geothermal reservoirs can be regarded as thoroughly established (D'Amore and Arnórsson, 2000) and have been extensively used in geothermal studies. Well MW-01 chemical results show that equilibrium between quartz and alkali feldspars and solution is attained in the Menengai geothermal well at an estimated temperature of 195°C from quartz and 191°C from Na/K (Table 3). There is relatively good conformity between both quartz and Na/K values, with an average difference of 4°C. Correlating geothermometer temperatures with temperatures from downhole logging (Figure 3), it can be argued that fluids inflowing from the shallower permeable horizons largely influence the discharge at the wellhead.

TABLE 3: Geothermometer temperatures for Menengai well MW-01

Sample no.	**592**	**593**	**594**	**595**	**596**	**597**	**598**	**599**	**600**	**601**	**602**	**603**
T_{qtz} (°C)	195	200	185	186	187	199	191	199	192	203	203	199
T_{NaK} (°C)	188	211	200	192	195	189	189	189	187	186	185	182

4.4 Integrated results

Loss of circulation of drilling fluid, pressure and temperature logs and CO_2 gas pressures indicate the existence of four main feed zones of varying temperatures in Menengai well MW-01. Geothermometers indicate that the liquid water in the well discharge is dominated by fluids withdrawn from the shallowest aquifer. It is also evident that gas pressures, predominantly CO_2, lower the boiling point of the fluids in the well, especially at the points or depth levels at which fluids enter the well. These have been taken as good indicators of feed zones.

5. AQUIFER FLUID COMPOSITION AND BOILING

5.1 Boiling

As pointed out earlier (see Section 4), boiling in well MW-01 occurs beyond the well bottom. The bottom-hole temperature during discharge is 265°C (flowing profile in Figure 3) but decreases as the fluid ascends due to boiling by depressurization and inflows from shallower feed zones. When the well is not discharging, the pressure at the bottom is 153 bars, corresponding to a boiling point for pure water of 343°C. The CO_2 partial pressure will lower the boiling point of the actual fluid relative to pure water, possibly by as much as 20°C. Therefore, the maximum reservoir temperature at the well bottom is around 320°C.

The discharged liquid indicates much lower temperatures (about 190°C) as deduced from the quartz and Na/K geothermometers. This large difference results from the effects of inflows from shallower, and therefore, cooler feed zones. The discharge enthalpy is higher than that of steam saturated water at the geothermometer temperatures. This may be the consequence of poor analytical data rather than an indication of 'excess' enthalpy. However, the enthalpy of the fluid from the deepest aquifers could indeed be in excess, as boiling is extensive in these aquifers, as indicated by pressures during shut-in and discharge.

Several reasons may be given for excess enthalpy of wet-steam well discharges, but two are probable in the case of Menengai well MW-01. The presence of a significant steam fraction in the initial aquifer fluid is one possibility. It is conceivable that the vapour present in the initial fluid as well as all vapour formed by depressurization boiling enters the well. If the well has both liquid and steam feeds, a steam cap may form by gravity segregation of water and steam, hence raising the discharge enthalpy. Studies have revealed that two-phase geothermal systems are hydrologically unstable (Arnórsson and D'Amore, 2000). The steam tends to rise faster than the water because of its lower density. The extent of this gravity segregation depends on the rock permeability. The steam fraction at each level in the reservoir depends on its rate of generation, condensation and permeability. The other possibility is the consequence of processes in the depressurization zone around the well resulting in phase segregation. As discussed by Arnórsson and Stefánsson (2005), such segregation is the consequence of the effects of capillary forces, the different flow properties of the two phases, water and steam, and relative permeability. The mass flow rate at each phase is determined by the relative permeability and the pressure gradient, which is generally different for the two phases, as well as the densities and viscosities of water and steam.

5.2 Aquifer fluid composition

It has been well established that knowledge of the composition and speciation of aquifer fluids in geothermal systems is crucial to understanding the source and evolution of these fluids and for characterizing the geothermal system. Procedures for calculating the chemical composition of aquifer fluids from the discharge enthalpy and the analysis of samples collected at the wellhead, based on a

reasonable set of assumptions, have been discussed extensively by Arnórsson et al. (2007) and Arnórsson et al. (2010). Several models have been proposed. The method chosen to compute aquifer fluid compositions, therefore, depends on the model selected to explain the cause of the excess enthalpy in the well. However, evaluation of aquifer chemistry for well MW-01 is complicated by the fact that the discharge is an admixture of many components from sub-systems with significantly different temperatures. In such a case, local equilibrium may or may not have been closely approached within all these sub-systems, and the selection of a single aquifer temperature is always a simplification of the real conditions in the geothermal system.

To calculate the chemical composition of the initial liquid and vapour in MW-01 aquifer, the relative contributions of the different processes to the excess discharge enthalpy and the initial vapour fraction of the aquifer fluid need to be evaluated. In the absence of such an assessment, composition of aquifer fluids has been calculated without basing it on a single temperature but rather from both the quartz equilibrium temperature and the bottom-hole temperature of 265°C during discharge.

In the present contribution, liquid enthalpy has been assumed for the discharge and two temperatures have been selected to calculate the aquifer liquid composition on that assumption, i.e. at the quartz equilibrium temperature and at 265°C. When using the lower reference temperature, it is effectively assumed that essentially all the fluid is derived from the shallowest feed zone at about 1050 m. The choice of 265°C is a minimum value for the two deepest feeds. In reality, the undisturbed temperature of the deep feed zones must be higher than 265°C, indicating that the discharge enthalpy is the product of higher fluid enthalpy from the deep feeds and lower fluid enthalpy from the shallower feeds. The primary data for these calculations are presented in Table 4 and the modelled aquifer liquid compositions in Table 5. The results of the two models differ significantly. Yet they are considered to give an indication of the component concentrations in the feed zones of MW-01. The WATCH speciation program of Arnórsson et al. (1982), version 2.4 (Bjarnason, 2010) was used for the above described calculations.

TABLE 4: Wellhead compositions

Water sample (ppm)		**Steam sample (mmol/kg)**	
pH/°C	6.3/20		
SiO_2	283	CO_2	1425
B	0.13	H_2S	3.5
Na	2364.5	H_2	14.4
Ca	0.9	CH_4	3.9
Mg	0.005	N_2	25.8
ΣCO_2	6589	O_2	0
SO_4	212.4	**Physical parameter**	
H_2S	37.4	Enthalpy 1158 kJ/kg	
Cl	774.8		

6. SCALING POTENTIAL

6.1 Background

The saturation state of the aquifer water in well MW-01 for calcite and amorphous silica has been assessed. These minerals are of major concern in relation to scale formation as their deposition to form scales can cause difficult operational problems and have serious economic consequences ranging from equipment damage and failure to power production. Different types of geothermal waters with varying chemistry are found in diverse geothermal areas around the world. The chemistry can also vary substantially even in different wells within the same geothermal field. The chemistry of these waters is influenced by several factors including the geology of the resource, temperature, pressure and the source of water. This, therefore, makes the understanding of the chemistry of the waters critical for successful utilization. According to Arnórsson (2000), assessment of changes in mineral saturation upon boiling and cooling of geothermal waters should always be made when geochemical data on fluid composition from exploration wells become available. This assessment should be updated as data from new wells become available and as more data accumulate during long term

production. This is essential in understanding the scaling potential of the waters and finding ways of solving it.

The chemical composition of geothermal waters depends primarily on temperature and the mineralogical composition of the geological formations of the reservoir. Different types of scales are found in various geothermal areas and, sometimes, even within the various wells of the same geothermal field. The major species of scale in geothermal waters typically include calcium carbonate minerals, amorphous silica and sulphide compounds (Stapleton, 2002). Calcite and silica deposits are the most frequent scale formation materials (Patzay et al., 2003). Calcite scaling is common in geothermal production wells while silica deposition is of concern if geothermal water cools sufficiently through boiling to make it amorphous silica supersaturated (Arnórsson, 2000). The saturation of calcite and amorphous silica at various temperatures have been computed for the fluid discharged from well MW-01, using the WATCH speciation program of Arnórsson et al. (1982) version 2.4 (Bjarnason, 2010) to predict their scale potential.

TABLE 5: Aquifer fluid compositions at the quartz equilibrium temperature and at 265°C; all concentrations are in ppm

	Temp (°C)	
Species	**191[a]**	**265[b]**
SiO_2	234.7	190.1
B	0.11	0.09
Na	1961.4	1588.5
K	179.8	145.6
Ca	0.75	0.6
Mg	0.004	0.003
SO_4	176.2	142.7
Cl	642.7	520.5
CO_2	14852.4	22495.0
H_2S	103.7	165.0
H_2	9.7	18.6
CH_4	11.8	22.6
N_2	37.7	72.6

[a] Quartz equilibrium temperature; [b]Selected temperature

6.2 Amorphous silica

The saturation state of well MW-01water with respect to amorphous silica was evaluated using the well chemical data for a selected sample. The sample selected had the least discrepancy between the geothermometers used. It is not known what the chemical composition of the fluid ascending in the well is below the shallowest feed zone. Above this feed it is, however, the same as that of the total discharge. During discharge, the temperature of the shallowest feed zone (1050 m depth) is 235°C. Figures 6 and 7 show amorphous silica saturation at lower temperatures produced by depressurization boiling from two reference temperatures, the measured temperature during discharge at the shallowest feed and the quartz equilibrium temperature. The results indicate that amorphous silica precipi-

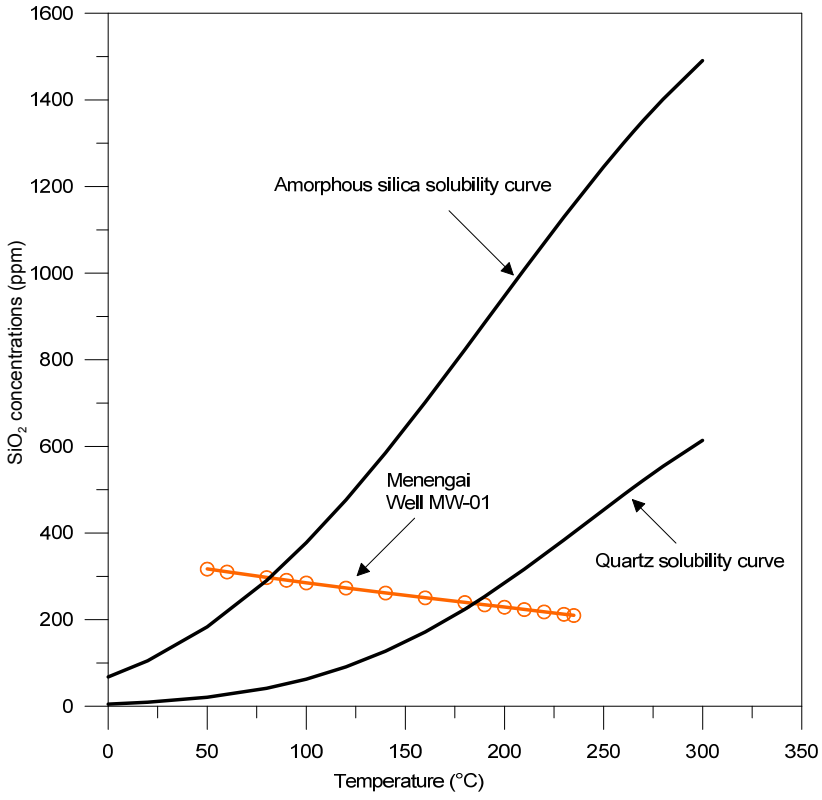

FIGURE 6: SiO_2 concentrations in MW-01 water during one step adiabatic boiling from measured bottom-hole temperature during discharge

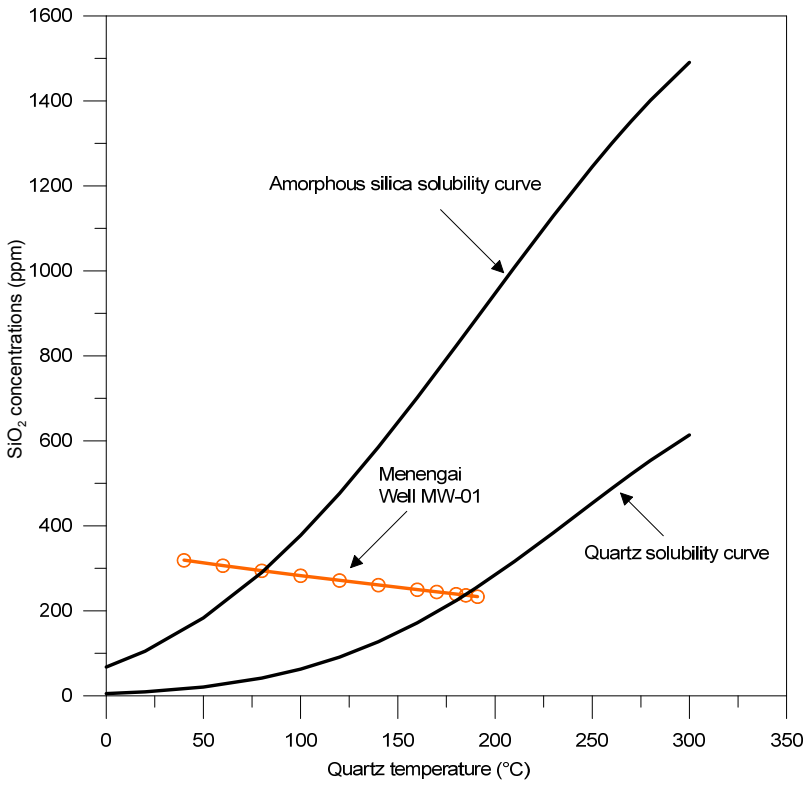

FIGURE 7: SiO_2 concentrations in MW-01 water during one step adiabatic boiling from quartz equilibrium temperature

tation will not be a problem, neither above the shallowest feed, nor at deeper levels. Amorphous silica saturation is not reached until the boiled water has cooled below 80°C, and below this temperature amorphous silica deposition rate is likely to be low for kinetic reasons. It should, however, be pointed out that the water at 235°C is quartz under-saturated. This could indicate that the silica analysis is in error and that the true concentration value is higher, unless the shallow feed at 1050 m depth is colder than the temperature measured during discharge. The solubility curves for both quartz and amorphous silica are based on solubility equations for the reaction $SiO_2 + 2H_2O = H_4SiO_4°$ (Gunnarsson and Arnórsson, 2000).

6.3 Calcite

Calcite is an abundant secondary mineral in drilled geothermal fields worldwide, implying that geothermal reservoir waters are generally calcite saturated (Arnórsson, 1989; Ellis and Mahon, 1977; Arnórsson, 1978; Giggenbach, 1980; Arnórsson et al., 1983). It is the most common carbonate scale in geothermal wells. Studies of deposits downhole have revealed that they begin to form at the depth level of first boiling (bubble point) where they tend to be most intense and the volume of deposit diminishes upwards (Arnórsson, 1989; Benoit, 1989). The solubility of calcium carbonate minerals in an aqueous solution at any particular temperature increases with increasing partial pressure of CO_2 (e.g. Arnórsson 1978; Fournier, 1985) as can be seen from the following reaction:

$$CaCO_{3,s} + 2H^+ = Ca^{+2} + CO_2 + H_2O \quad (1)$$

The main problem in assessing calcite scale potential in the entire wellbore of Menengai well MW-01 is that the discharge is a mixture of fluids from four feed zones. One of these zones appears to be small and the two deep feeds are closely spaced so it appears to be a reasonable approximation to treat them as one feed zone. Therefore, the discharge is essentially a mixture of fluid from two feeds. Data on downhole temperatures are not available for thermally stabilized wells. For this reason, it is not possible to evaluate undisturbed aquifer temperatures in the two main feed zones. Due to these limitations, three scenarios have been selected to calculate calcite saturation state in MW-01. Since all these scenarios use the total discharge compositions but select different temperatures, i.e. quartz equilibrium temperature (191°C) and measured temperatures during discharge at the depth level of the two major feeds (235 and 265 °C), the points fall on the same curve. The results are shown by the graph in Figure 8. For these calculations, boiling was taken to be caused by depressurization.

First, the most reliable scenario will be discussed, the one with the starting temperature of 235°C that corresponds to the fluid just above the shallowest feed zone. For this scenario, the results indicate that the water is rather strongly over-saturated, by close to 1.3 log units assuming maximum degassing. At the quartz reference temperature, calcite is over-saturated by 1.0 log units. All the points fall on the same curve because they are based on the same flowing fluid enthalpy and composition. The lower over-saturation at 265°C can be attributed to the higher CO_2 calculated concentration in the liquid water at this temperature rather than at 235°C, or 19,600 compared to 1,400 ppm. The CO_2 concentration value at 265°C will be high because it assumes that only liquid water exists at this temperature but, in reality, both liquid and vapour phases are present. By selecting both higher temperature and higher discharge enthalpy for the deepest feed zones, a greater over-saturation with respect to calcite is obtained.

Subsequent to boiling, a substantial reduction in CO_2 partial pressure occurs as CO_2 partitions into the steam phase (Figure 9). The result is a decrease in the solubility of calcium carbonate. The pH of the water (see Figure 10) as well as the dissociation constant for aqueous carbon dioxide (H_2CO_3) and bicarbonate (HCO_3^-) also increase with degassing of the water. This leads to an increase in the concentrations of carbonate (Figure 11) which is largely responsible for the over-saturation of the solution with respect to calcite. On the other hand, the chemical results indicate a deficiency of calcium in well MW-01 water. The low calcium

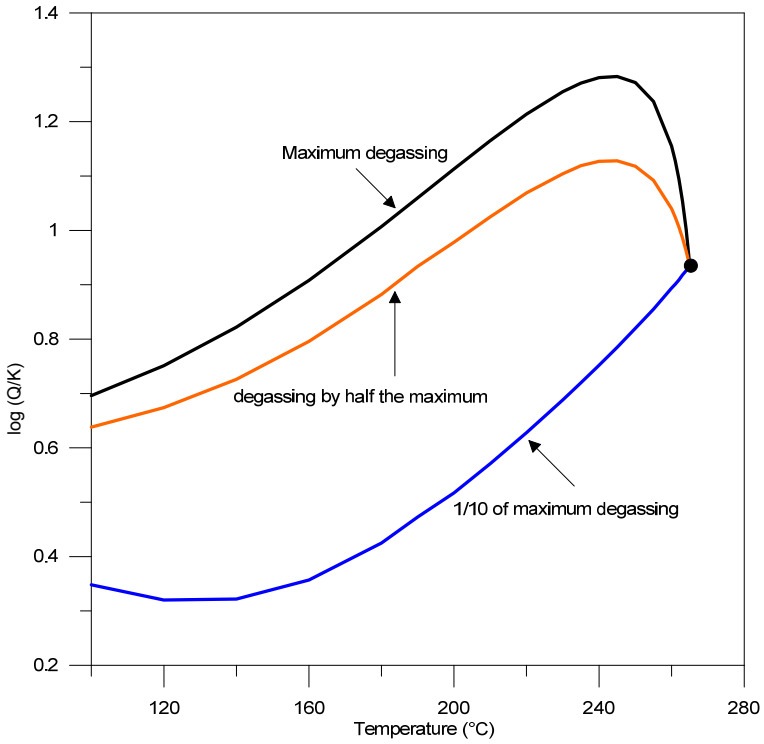

FIGURE 8: Changes in calcite saturation during one step adiabatic flashing at various degassing coefficients

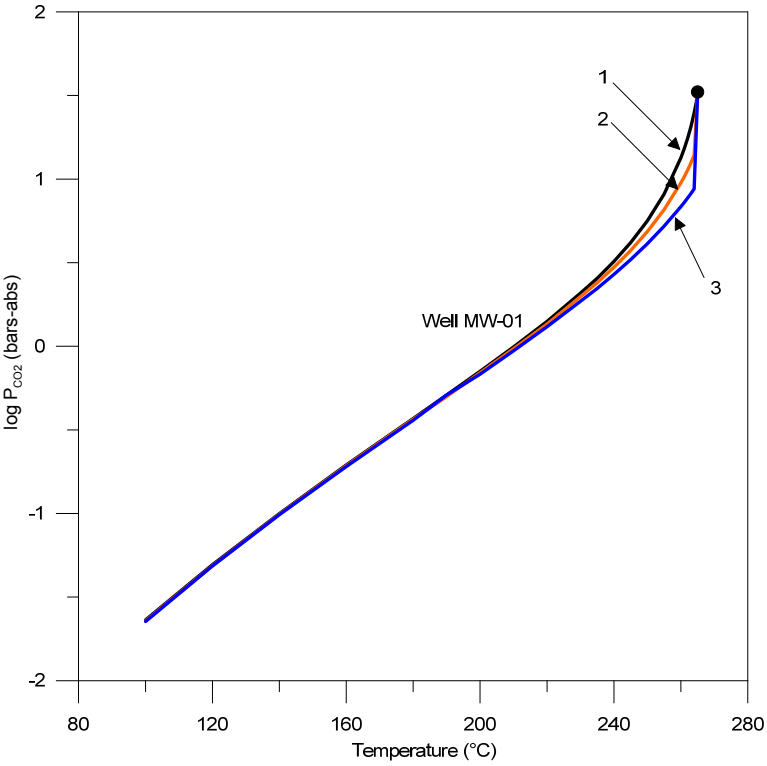

FIGURE 9: Changes in CO_2 partial pressures during adiabatic boiling in well MW-01; curves 1, 2 and 3 represent maximum, ½ and 1/10 of maximum degassing, respectively

values in the discharge may be due to calcite deposition which results from the removal of a substantial part of calcium from the water in the aquifer. The reason for an increased concentration of free calcium ions (Ca^{2+}) during flashing of the water may be due to the dissociation of $CaHCO_3^+$ and steam loss. Combined activities of CO_3^{2-} and Ca^{2+} would, therefore, be sufficient to produce calcite over-saturated solution in the well as seen in Figure 8.

The results depicted in Figure 8 are taken to indicate that calcite scaling is likely to be a problem in the wellbore of MW-01. The over-saturation is, however, slightly lower assuming the solution degasses by half the maximum but seems to behave much differently for a much lower degassing, i.e. a tenth of the maximum. The graph corresponding to this least degassing of the aquifer water appears to show an increasing calcite over-saturation at the reference temperature, but falls sharply upon boiling of the water. Nonetheless, all the graphs indicate strong calcite over-saturation in the flashing geothermal water in well MW-01. To substantiate the likelihood of strong calcite scaling, it is necessary to have very accurate data on both pH and total carbonate carbon in water samples and on CO_2 in steam samples. Further, both types of samples need to be collected from a vapour separator at the same pressure.

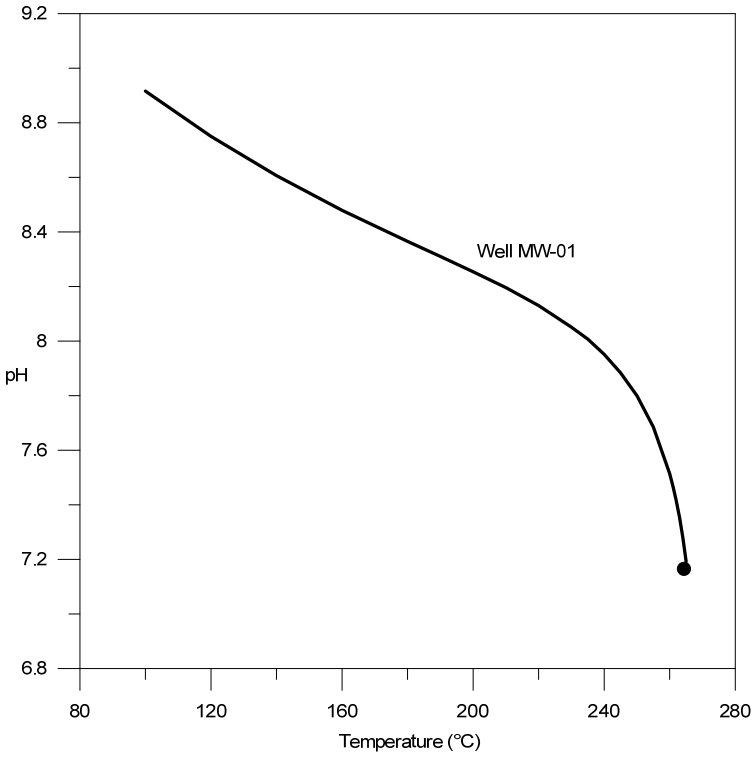

FIGURE 10: Variation in pH during one step adiabatic flashing of well MW-01 water assuming maximum degassing

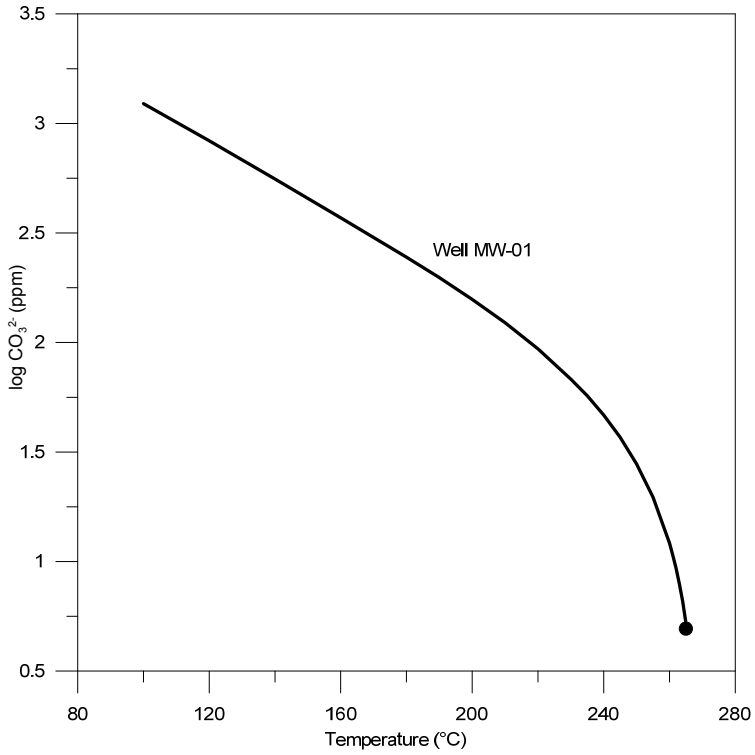

FIGURE 11: The variation in CO_3^{2-} content during one step adiabatic boiling assuming maximum degassing

7. STEAM QUALITY

The effect of the gas content of aqueous fluids in well MW-01 on the boiling point has been discussed in previous chapters of this report.

The purpose of this section is to consider the possible effects of gases on the utilization of geothermal steam from well MW-01 for electric power generation. Detailed study will, however, be necessary to quantify these effects.

The quality of steam can considerably affect the efficiency and reliability of steam-powered equipment. Dry steam or steam of 100% quality consists solely of water vapour, while qualities less than 100% indicate contents of impurities, moisture and gases which passed into the steam during the process of flashing and separation of geothermal fluid steam and water phases. Well MW-01 contains significant amounts of non-condensable gases and high CO_2 concentrations, as inferred by the chemical compositions of the discharged fluids. The non-condensable gases include CH_4, H_2, NH_3, and N_2. These gases and CO_2 decrease the vacuum at the turbine outlet and thereby the turbine efficiency. The characteristics of a geothermal source, therefore, have an influence on the choice of systems to be used in power plants. Geothermal gas levels are highly variable and site specific. Vorum and Fritzler (2000) summarized the practical problems associated with elevated levels of gases in geothermal steam power systems. Highlighted below are some of their findings:

- The gases reduce heat transfer efficiency of the power plant condensers. The primary effect of this is to increase the condensing operating pressure, which reduces turbine power output. Consequently, overcoming the gas effects requires bigger condensers with greater total heat transfer area and, hence, higher costs.
- The gases contribute a higher partial pressure that adds to the gas pressure on the turbine. If the gas removl systems (commonly vacuum equipment) underperform, which has the effect of an under-designed condenser, then the power turbine backpressure increases.
- Non-condensable gases contain lower recoverable specific energy than does steam. The gases dilute the geothermal steam and reduce gross turbine output in the power plant.
- Acid gases such as CO_2 and H_2S are highly water soluble and contribute to corrosion problems in piping and equipment that have contact with steam and condensate.

In this chapter, emphasis is laid on the CO_2 gas component in Menengai well MW-01 because of its dominant concentrations, but the results are broadly applicable to other gases by way of extrapolation. Chemical results show that concentrations of CO_2 in steam at the wellhead (8.7 bars) constitute about 2.2 moles/kg of steam. This translates to around 4% by volume of CO_2 in the vapour at the wellhead. This implies that the high gas content in the steam deteriorates its quality.

D'Amore and Celati (1983) published a technique for computing the steam quality in the aquifer through calculations of the molar fractions in the steam phase of the chemical species in the aquifer from the wellhead compositions. However, this method may not be applicable in the case of a well producing fluid with high gas content like well MW-01. Keeping this limitation in mind, only the formula for estimating the fraction of steam is to assess the ratio of steam to water in the total discharge. The main challenge with the discharge from well MW-01 though is that it constitutes fluids withdrawn from two major aquifers, likely of significantly varying temperatures as has been elaborated in the previous chapter. The steam fraction is, therefore, calculated based on the conditions at the shallowest aquifer since the fluid at this depth is that discharged at the wellhead. Taking the fluid at this depth as the initial fluid, i.e. fluid beyond the depressurization zone around the well, the steam fraction can be computed from the following formula:

$$\mathrm{x}^{d,v} = \frac{h^{d,t} - h^{d,l}}{h^{d,v} - h^{d,l}} \tag{2}$$

where $\mathrm{x}^{d,v}$ is the vapour fraction of the well discharge by mass, and $h^{d,t}$, $h^{d,l}$ and $h^{d,v}$ represent the discharge enthalpy, the enthalpy of discharged liquid and that of saturated steam, respectively. Both $h^{d,l}$ and $h^{d,v}$ values can be obtained from steam tables.

8. DISCUSSION

8.1 Comparison with Olkaria

Olkaria geothermal field, located to the south of Menengai at a distance of about 100 km, has been under exploitation for over two decades now. Many studies on the geothermal system have been conducted and the findings published. Comparing the two systems is somewhat constrained by the fact that the results under consideration for Menengai are based on only one well that has yet to thermally stabilize, as opposed to the over-time exploitation in Olkaria. However, despite this limitation, some parallels can still be drawn and notable differences observed from the two geothermal systems, the one in Olkaria and that in Menengai, from geochemical evidence and flow tests carried out in well MW-01.

In the Olkaria geothermal system, the flashed water discharged from the wells is of Na-Cl or Na-HCO_3 type with the most abundant dissolved constituent being CO_2 (Karingithi et al., 2010). Variations exist in the chemistry of the different well fields within the greater Olkaria geothermal system. Olkaria West and Domes have high CO_2 concentrations which are mainly source controlled. Menengai compares somewhat with these well-fields, going by the high CO_2 concentrations in well MW-01 discharge, although they are much higher. Both geothermal systems seem to be low in calcium concentrations.

Higher discharge enthalpies, considered excess, are reported for many Olkaria wells, some close to 2600 kJ/kg (Karingithi el al., 2010). The discharge enthalpy from well MW-01 in Menengai is relatively low. This is possibly due to the large contribution to the discharge by fluids emanating from the shallowest aquifer of quite low temperature. Low temperature fluids appear to be found at deeper horizons in Menengai as opposed to Olkaria. This would imply deeper production casing for wells drilled in Menengai for effective harnessing of steam.

8.2 Environmental issues

Geothermal energy is widely considered as a clean energy source because of its minimal impact on the environment. However, several issues relating to the chemistry of geothermal fluids are required to be considered and explored to ensure safe and economic energy production from geothermal fields. The discussion in this section is only limited to concerns over emissions of important greenhouse gases (in particular, CO_2) from discharged fluids from well MW-01. This has been necessitated by the high CO_2 concentrations both in the gas and liquid phases of the well discharge. The aim of this discussion is not to quantify the effects but rather to point out the need to carry out an assessment on environmental effects. While studies on CO_2 emissions from geothermal/volcanic systems have established that huge quantities of the gas are released naturally and, in many cases, natural emissions far exceed emissions from geothermal power production (Seward and Kerrick, 1996; Delgado et al., 1998; Bertani and Thain, 2002), it is of importance to assess and monitor these emissions.

Menengai well MW-01 chemical results indicate that the vapour discharged contains about 1.75 mol CO_2/kg steam given an operating pressure of 6 bars-abs. This would translate to about 3.2 % by volume of CO_2 in a kilogram of steam. In addition, the water has high dissolved CO_2 content as well.

9. SUMMARY AND CONCLUSIONS

A combined examination of the well lithology, pressure and temperature logs, flow tests and geochemical data provides valuable information on the geothermal system penetrated by the well. The information obtained from well MW-01 is of major importance in several ways. Decisions on other

exploration wells, both vertical and deviated, can immensely benefit from and be guided by the knowledge gained from the characteristics of this well. Information crucial to determining the production casing depth and spacing of subsequent drill holes can also be obtained from the findings from the first exploration wells already sunk.

Mixing of cooler inflows from shallower aquifers with hotter fluids from deeper feeds in the well is evident from the low quartz and Na/K equilibrium temperatures in relation to the measured temperatures. Four (4) feed zones have been identified in well MW-01. However, the dominant feeds have been taken to be two: the shallower feed of relatively low temperature and the deeper feed of high temperatures. The temperature and composition of the fluids at each feed zone is not known. Modelling of aquifer fluid compositions is thereby complicated by this significant difference in temperatures in the main aquifers. It is not possible, in view of these limitations, to select a single source temperature for calculating aquifer fluid compositions.

Gas content in the fluid, as is evident from the chemical results of well MW-01, can affect well performance due to resulting gas pressures. High gas partial pressures lower the boiling point of the water in geothermal wells, causing boiling to occur at a higher pressure, that is, deeper in the well. From the pressure measurements during well shut-in and the boiling point curve with depth of pure water for well W-01, it is possible that high temperatures of up to 320°C exist at the well bottom, taking into account the gas partial pressures (predominantly CO_2). Moreover, pressure measurements during discharge indicate a two-phase flow in this well from the well bottom. This would imply that the temperatures for the shallowest feed zones influencing the equilibrium temperatures for the discharged liquid could be quite low.

Chemical results indicate that the aquifer water is of Na-HCO_3 type with relatively high Cl values (>500 ppm). The most abundant dissolved component in the aquifer fluid is CO_2. This high CO_2 appears to be influenced by magmatic flux rather than by equilibrium with mineral assemblages. The high CO_2, by its flux to the hydrothermal fluids, also contributes enormously to high concentrations of carbonate ions largely responsible for over-saturating the solution with calcite. This may also explain the low calcium values in the discharged water. Much of it may have been removed from the solution by calcite precipitation.

Good sampling and accurate and precise analysis of the well fluids cannot be overemphasized. Interpretation of chemical data can be severely hampered by the quality of analytical data. Calculated pH used in this report was based on the assumption that possible degassing of the water occurred between sample collection and pH measurements, hence raising the pH of the solution. This assumption was based on the highly dissolved content of the CO_2 gas. The pH calculations were done using the WATCH program. Corrections for possible silica polymerization were not done and, therefore, not accounted for in this report.

In conclusion, it is important to note that the well has not reached thermal stabilization. Temperatures of the undisturbed aquifers cannot, therefore, be ascertained. Additional chemical data, and of good quality, are required to affirm these findings. This would also give a good prediction of calcite scaling potential of the flashing geothermal waters in Menengai well MW-01.

ACKNOWLEDGEMENTS

My great and sincere appreciation to my supervisor, Professor Stefán Arnórsson for his invaluable support, advice and guidance in the preparation of this project paper; I am honoured to have been his student. I am most grateful to Dr. Ingvar B. Fridleifsson, Director, United Nations University Geothermal Training Programme (UNU-GTP) for offering me the opportunity to participate in the six months programme and to Lúdvík S. Georgsson, Deputy Director, UNU-GTP for his prized assistance

throughout the entire programme. Many thanks to UNU-GTP staff: Thórhildur Ísberg, Ingimar G. Haraldsson and Markús A.G. Wilde for their kindness, care and support towards making the studies and the project work a success and the stay in Iceland delightful. I am thankful to Rósa S. Jónsdóttir for her kind assistance with papers and reference materials during the study period. The entire Orkugardur community is much appreciated for diverse contributions towards the training and a favourable stay in Iceland. I am grateful to the UNU-GTP Fellows for a fruitful time together and the friendships made. Special thanks to my employer, Geothermal Development Company Ltd. (GDC) for affording me the chance to attend the UNG-GTP programme and for availing me with the data used in this report.

My deepest appreciation goes to my wife for her sacrifice and support during the period I have been away from home. This report is dedicated to her. Finally, to God, be all the praise and glory for the successful completion of the training programme.

REFERENCES

Arnórsson, S., 1978: Precipitation of calcite from flashed geothermal waters in Iceland. *Contrib. Mineral. Petrol., 66,* 21-28.

Arnórsson, S., 1985: Gas pressures in geothermal systems. *Chemical Geology, 49,* 319-328.

Arnórsson, S., 1989: Deposition of calcium carbonate minerals from geothermal waters - theoretical considerations. *Geothermics, 18,* 33-39.

Arnórsson, S., 2000: Mineral saturation. In: Arnórsson, S. (editor), *Isotopic and chemical techniques in geothermal exploration, development and use. Sampling methods, data handling, interpretation.* International Atomic Energy Agency, Vienna, 241-266.

Arnórsson, S., Angcoy, E., Bjarnason, J.Ö., Giroud, N., Gunnarsson, I., Kaasalinen, H., Karingithi, C., Stefánsson, A., 2010: Gas chemistry of volcanic geothermal systems. *Proceedings of the World Geothermal Congress 2010, Bali, Indonesia,* 6 pp.

Arnórsson, S., Bjarnason, J.Ö., Giroud, N., Gunnarsson, I., and Stefánsson, A., 2006: Sampling and analysis of geothermal fluids. *Geofluids, 6,* 203-216.

Arnórsson, S., and D'Amore, F. 2000: Estimation of aquifer steam fraction. In: Arnórsson, S. (editor), *Isotopic and chemical techniques in geothermal exploration, development and use. Sampling methods, data handling, interpretation.* International Atomic Energy Agency, Vienna, 267-308.

Arnórsson, S., Gunnlaugsson, E., and Svavarsson, H., 1983: The chemistry of geothermal waters in Iceland II. Mineral equilibria and independent variables controlling water compositions. *Geochim. Cosmochim. Acta, 47*, 547-566.

Arnórsson, S., Sigurdsson, S., and Svavarsson, H., 1982: The chemistry of geothermal waters in Iceland I. Calculation of aqueous speciation from 0° to 370 °C. *Geochim. Cosmochim. Acta, 46,* 1513-1532.

Arnórsson, S. and Stefánsson, A., 2005: Wet-steam well discharges II. Assessment of aquifer fluid compositions. *Proceedings of the World Geothermal Congress 2005, Antalya, Turkey,* 11 pp.

Arnórsson, S., Stefánsson, A., Bjarnason, J.Ö., 2007: Fluid-fluid interaction in geothermal systems. *Reviews in Mineralogy & Geochemistry, 65,* 259-312.

Benoit, W.R., 1989: Carbonate scaling characteristics in Dixie Valley, Nevada geothermal wellbores. *Geothermics, 18-1/2,* 41-48.

Bertani, R. and Thain, I., 2002: Geothermal power generating plant CO_2 emission survey. *IGA News, 49,* 1-3.

Bjarnason, J.Ö., 2010: *The speciation program WATCH, version 2.4, user's guide*. Iceland Water Chemistry Group, Reykjavík, 9 pp.

D'Amore, F., and Arnórsson, S., 2000: Geothermometry. In: Arnórsson, S. (editor), *Isotopic and chemical techniques in geothermal exploration, development and use. Sampling methods, data handling, interpretation.* International Atomic Energy Agency, Vienna IAEA, Vienna, 152-199.

D'Amore, F., and Celati, C., 1983: Methodology for calculating steam quality in geothermal reservoirs. *Geothermics, 12,* 129-140.

Delgado, H., Piedad-Sanchez, N., Galvian, L., Julio, P., Alvarez, J.M., Cardenas, L., 1998: CO_2 flux measurements at Popocatepetl volcano II. Magnitude of emissions and significance (abstract). *EOS Trans. Am. Geopys. Union, 79,* 926.

Ellis, A.J., and Mahon, W.A.J., 1977: *Chemistry and geothermal systems*. Academic Press, New York, USA, 392 pp.

Fournier, R.O., 1985: The behaviour of silica in hydrothermal solutions. *Rev. Econ. Geology, 2,* 45-61.

Fournier, R.O., and Potter, R.W. II, 1982: A revised and expanded silica (quartz) geothermometer. *Geoth. Res. Council Bull., 11-10*, 3-12.

GDC, 2011: *Menengai well locations map.* GDC database.

Geotermica Italiana Srl., 1987: *Geothermal reconnaissance survey in the Menengai- Bogoria area of the Kenya Rift Valley.* UN (DTCD)/GOK.

Giggenbach, W.F., 1980: Geothermal gas equilibria. *Geochim. Cosmochim. Acta, 44*, 2021-2032.

Grant, M.A, and Bixley, P.F., 2011: *Geothermal reservoir engineering* (2nd edition). Elsevier, Academic Press, 378 pp.

Grant, M.A., Bixley, P.F., and Donaldson, I.G., 1983: Internal flows in geothermal wells: Their identification and effect on the wellbore temperature and pressure profiles. *Soc. Pet. Engin. J., 23-1,* 168-176.

Jones, W.B., and Lippard, S.J., 1979: New age determination and geology of Kenya rift – Nyanzian rift junction, West Kenya. *J. Geol. Soc. London, 136,* 63.

Karingithi, C.W, Arnórsson, S., and Grönvold, K., 2010: Processes controlling aquifer fluid compositions in the Olkaria geothermal system, Kenya. *J. Volcanol. & Geoth. Res., 196,* 57-76.

Lagat, J., Mbia, P., and Mutria, C., 2010: *Menengai prospect: Investigations for its geothermal potential.* GDC internal report, 64 pp.

Leat, P.T., 1984: Geological evolution of the trachytic volcano Menengai, Kenya Rift Valley. *J. Geol. Soc. London, 141,* 1057-1069.

Leat, P.T., 1985: Discussion on the geological evolution of the trachytic caldera volcano Menengai, Kenya Rift Valley. *J. Geol. Soc. London, 142-4,* 711-712.

Leat, P.T., Macdonald, R., and Smith, R.L., 1984: Geochemical evolution of Menengai, Kenya Rift Valley. *J. Geophys. Res., 89,* 8571-8592.

Macdonald, R., Navarro, J.M., Upton, B.G. J., and Davies, G.R., 1994: Strong compositional zonation in peralkaline magma: Menengai, Kenya Rift Valley. *J. Volc. Geotherm. Res.*, *60,* 301-325.

Mungania, J., and Lagat, J., (editors), Mariita, N.O., Wambugu, J.M., Ofwona, C.O., Kubo, B.M., Kilele, D.K., Mudachi, V.S., Wanjie, C.K., and Korio, R.K., 2004: *Menengai volcano: Investigations for its geothermal potential.* KenGen internal report, 93 pp.

Ofwona, C., Omenda, P., Mariita, N., Wambugu, J., Mwawongo, G., and Kubo, B., 2006: *Surface geothermal exploration of Korosi and Chepchuk prospects*. KenGen internal report, 44 pp.

Omenda, P.A., Onacha, S.A., and Ambusa, W.J., 1993: Geological setting and characteristics of the high temperature geothermal systems in Kenya. *Proceedings of the 15th New Zealand Geothermal Workshop, Geothermal Institute, New Zealand,* 161-167.

Patzay, G., Karman, H.F., and Pota, G., 2003: Preliminary investigations of scaling and corrosion in high enthalpy geothermal wells in Hungary. *Geothermics, 32,* 627-638.

Riaroh, D., and Okoth, W., 1994: The geothermal fields of the Kenya rift. *Tectonophysics, 236,* 117-130.

Seward, T.M., and Kerrick, D.M., 1996: Hydrothermal CO_2 emissions from the Taupo volcanic zone, New Zealand. *Earth Planet. Sci. Lett., 139,* 105-113.

Simiyu, S.M., 2010: Status of geothermal exploration in Kenya and future plans for its development. *Proceedings of the World Geothermal Congress 2010, Bali, Indonesia*, 11 pp.

Simiyu, S.M., and Keller, G.R., 1997: An integrated analysis of the lithospheric structure across the east African plateau based on gravity analysis and recent seismic studies. *Tectonophysics, 278,* 291-313.

Simiyu, S.M., and Keller, G.R., 2001: An integrated geophysical analysis of the upper crust of the southern Kenya rift. *Geophys. J. Int., 147,* 543-561.

Stapleton, M., 2002: Scaling and corrosion in geothermal operation. *GeoChemical Services – PowerChem Technology,* 7 pp.

Stefánsson, V., and Björnsson, S., 1982: Physical aspects of hydrothermal systems. *Geodynamics Series, 8,* 123-145.

Vorum, M., and Fritzler, E.A., 2000: *Comparative analysis of alternative means of removing noncondensable gases from flashed-steam geothermal power plants.* National Renewable Energy Laboratory, report NREL/SR-550-28329, 69 pp.

Williams, L.A.J., Macdonald, R., and Chapman, G.R., 1984: Late Quaternary caldera volcanoes of the Kenya Rift Valley. *J. Geophys. Res., 89,* 8553-8570.

Young, P., Maguire, P., Laffoley, A., and Evans J., 1991: *Geophys. J. Int., 105,* 665-674.